

## Accepted Manuscript

Three-Dimensional Cobalt(II) and Cadmium(II) MOFs Containing 1,4-Naphthalenedicarboxylate: Catalytic Activity of Cd-MOF

In-Hwan Choi, Youngmee Kim, Do Nam Lee, Seong Huh

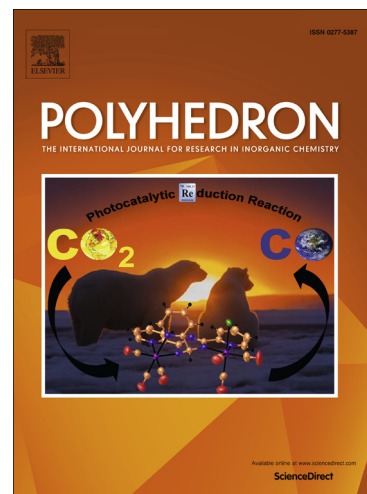
PII: S0277-5387(15)00772-X  
DOI: <http://dx.doi.org/10.1016/j.poly.2015.12.022>  
Reference: POLY 11721

To appear in: *Polyhedron*

Received Date: 10 November 2015  
Accepted Date: 11 December 2015

Please cite this article as: I-H. Choi, Y. Kim, D.N. Lee, S. Huh, Three-Dimensional Cobalt(II) and Cadmium(II) MOFs Containing 1,4-Naphthalenedicarboxylate: Catalytic Activity of Cd-MOF, *Polyhedron* (2015), doi: <http://dx.doi.org/10.1016/j.poly.2015.12.022>

This is a PDF file of an unedited manuscript that has been accepted for publication. As a service to our customers we are providing this early version of the manuscript. The manuscript will undergo copyediting, typesetting, and review of the resulting proof before it is published in its final form. Please note that during the production process errors may be discovered which could affect the content, and all legal disclaimers that apply to the journal pertain.



## Three-Dimensional Cobalt(II) and Cadmium(II) MOFs Containing 1,4-Naphthalenedicarboxylate: Catalytic Activity of Cd-MOF

In-Hwan Choi,<sup>a</sup> Youngmee Kim,<sup>b</sup> Do Nam Lee,<sup>\*c</sup> and Seong Huh<sup>\*a</sup>

<sup>a</sup>Department of Chemistry and Protein Research Center for Bio-Industry, Hankuk University of Foreign Studies, Yongin 17035, Korea. Fax: +82-31-330-4566 E-mail: shuh@hufs.ac.kr

<sup>b</sup>Department of Chemistry and Nano Science, Ewha Womans Univeristy, Seoul 03760, Korea.

<sup>c</sup>Division of General Education (Chemistry), Kwangwoon Univeristy, Seoul 01897, Korea. Fax: +82-2-940-5677 E-mail: donamlee@hanmail.net

### Abstract

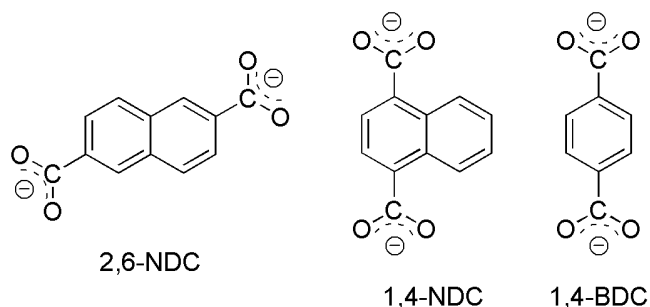
Three-dimensional (3D) cobalt(II) and cadmium(II) metal-organic frameworks bearing rigid 1,4-naphthalenedicarboxylate (1,4-NDC) linkers were prepared and their solid-state structures were characterized by X-ray crystallography. Both Co-MOF and Cd-MOF exhibited isostructural frameworks. 1,4-NDC ligands bridge the metal ions in chelating/bridging and simple bridging modes to form a 1D chains, and these 1D chains are interconnected by 1,4-NDC to form 3D frameworks with the formula of  $[M_2(1,4-NDC)_2(DMF)_2]$  ( $M = Co^{II}$  or  $Cd^{II}$ ). The as-prepared Cd-MOF was found to be catalytically active for the cyanosilylation reaction of aromatic aldehydes with nitro substituent in varying positions in the presence of trimethylsilyl cyanide to afford cyanohydrin trimethylsilyl ethers in a shape and size selective manner. The catalytic reaction is thought to have mainly occurred inside the Cd-MOF micropores which were generated through the partial dissociation of DMF ligands near the surfaces of Cd-MOF, where openly accessible coordination sites are available once the labile DMF ligands dissociate from  $Cd^{II}$  ions. The as-prepared Co-MOF did not exhibit catalytic activities for the same reaction.

**Keywords:** Metal-organic framework; 1,4-Naphthalenedicarboxylate; MOF catalysis; Cyanosilylation; Shape selectivity

## 1. Introduction

Since the first report of MOF-5 by Yaghi and coworkers [1], a large number of metal-organic frameworks have been disclosed. The chemical functionalities of the interior surfaces of MOFs are often strongly dependent on the type and nature of the polytopic organic bridging linkers which effectively interconnect different metal ion-based nodes [2]. The geometry and symmetry of these organic bridging linkers also influence the final topological networks of the resultant MOFs. Among the known ditopic organic bridging linkers, 2,6-naphthalenedicarboxylate (2,6-NDC) has often been employed as the bridging linker because it is commercially available and its geometry and molecular dimension are adequate for the production of novel MOF structures: In-MOF [3] with an anionic framework, Zn-MOFs (IRMOF-8 [4]), Cr-MOF [5] with MIL-101 topology,  $[M_3(2,6-NDC)_3(DMF)_4]_n$  [6] type of MOFs with  $Mn^{II}$ ,  $Fe^{II}$ , and  $Co^{II}$  ions, Mg-MOF (TUDMOF-2 and TUDMOF-3) [7], Cd-MOF with an additional 4-pyridinecarboxylate linker [8], Al-MOF (MIL-69) [9], and MOFs containing rare-earth elements such as  $Eu^{III}$ ,  $Tb^{III}$ , and  $Ce^{III}$  [10].

In contrast, the commercially available geometrical isomer, 1,4-naphthalenedicarboxylate (1,4-NDC), was less explored for the preparation of MOFs, presumably because 1,4-NDC has a much shorter dimension of two carboxylate groups than 2,6-NDC (Scheme 1). Despite its smaller dimension of two carboxylate groups which will bind two different metal ion centers, the perfectly linear angle between these two carboxylate groups compared to 2,6-NDC will benefit the generation of new topologically interesting MOF systems. The backbone structure of 1,4-NDC is exactly the same as that of the more commonly used 1,4-benzenedicarboxylate (1,4-BDC), which is a bridging linker found in MOF-5. Nevertheless, the extra phenyl ring in 1,4-NDC usually leads to different secondary building units (SBUs) and framework structures compared to the MOFs prepared from 1,4-BDC. A few examples of MOF contain 1,4-NDC without other ditopic N-donor co-ligands:  $Zn_6(1,4-NDC)_5(OH)_2(DMF)_2 \cdot 4DMF$  containing hexanuclear SBU (MOF-48) [11],  $Al(OH)(1,4-NDC)$  of MIL-53 topology [12],  $In(OH)(1,4-NDC) \cdot 2H_2O$  and  $HIn(1,4-NDC)_2 \cdot 2H_2O \cdot 1.5DMF$  [13]. Therefore, we predicted that new functional MOFs based on 1,4-NDC linkers with various metal ions would be possible.



Scheme 1. Structural comparison of 2,6-NDC, 1,4-NDC, and 1,4-BDC anionic ditopic linkers.

MOFs can be utilized as efficient heterogeneous catalytic systems when either Lewis acidic metal centers or Lewis acidic/basic functional ligands act as catalytic sites for organic transformations. Generally, the Lewis acidic metal centers are available due to the presence of openly accessible metal sites or defects in the frameworks [14]. There are several excellent review articles summarizing recent MOF-based catalytic systems for various organic transformations [15-17]. One of the most valuable MOF-based catalytic systems may be the cyanosilylation reaction between aldehydes and trimethylsilyl cyanide because the resulting products, cyanohydrins, are very useful intermediate compounds for fine chemicals and pharmaceuticals [18, 19].

In this report, we present two isostructural 1,4-NDC-based three-dimensional (3D) MOFs: Co-MOF and Cd-MOF. Co-MOF was obtained as very small single crystals while Cd-MOF was hierarchically grown as single crystals. The crystal structures of both 3D MOFs and the shape-selective catalysis of Cd-MOF for cyanosilylation reaction of aromatic aldehydes are also reported.

## 2. Experimental

### 2.1. General Methods

1,4-Naphthalenedicarboxylic acid (1,4-H<sub>2</sub>NDC) was purchased from TCI. All other commercially available starting materials and solvents were purchased from Sigma-Aldrich and TCI and were used without further purification.

### 2.2. Preparation of [Co<sub>2</sub>(1,4-NDC)<sub>2</sub>(DMF)<sub>2</sub>]

A mixture of  $\text{Co}(\text{NO}_3)_2 \cdot 6\text{H}_2\text{O}$  (0.145 g, 0.5 mmol) 1,4- $\text{H}_2\text{NDC}$  (0.216 g, 1.0 mmol) dissolved in 10 mL of DMF was sealed in a Teflon-lined high pressure bomb and stored at 130 °C for 48 h. The mixture was cooled to room temperature and the violet colored crystals were retrieved by filtration and washed with DMF. The crystals were air-dried overnight (0.160 g, 46%). Anal. calcd. for  $\text{C}_{30}\text{H}_{26}\text{Co}_2\text{N}_2\text{O}_{10}$  (692.39): C, 52.04; H, 3.78; N, 4.05. Found: C, 51.94; H, 3.93; N, 4.08.

### 2.3. Preparation of $[\text{Cd}_2(1,4\text{-NDC})_2(\text{DMF})_2]$

A mixture of  $\text{Cd}(\text{NO}_3)_2 \cdot 4\text{H}_2\text{O}$  (0.154 g, 0.5 mmol) 1,4- $\text{H}_2\text{NDC}$  (0.216 g, 1.0 mmol) dissolved in 10 mL of DMF was sealed in a Teflon-lined high pressure bomb and stored at 130 °C for 48 h. The mixture was cooled down to room temperature and the ivory colored crystals were retrieved by filtration and washed with DMF. The crystals were air-dried overnight (0.204 g, 60%). Anal. calcd. for  $\text{C}_{30}\text{H}_{26}\text{Cd}_2\text{N}_2\text{O}_{10}$  (799.33): C, 45.08; H, 3.28; N, 3.50. Found: C, 44.67; H, 3.21; N, 3.70.

### 2.4. Cyanosilylation of Aldehydes

A mixture of the as-prepared Cd- MOF catalyst (0.020 g, 0.0125 mmol), an aldehyde of choice (1.0 mmol, 4-nitrobenzaldehyde 0.151 g; 3-nitrobenzaldehyde 0.151 g; 2-nitrobenzaldehyde 0.151 g) and trimethylsilyl cyanide (0.125 mL, 1.0 mmol) in dry toluene (10 mL) was heated at 50 °C with constant stirring for 72 h. After cooling to room temperature, the MOF solids were filtered off and the filtrate was evaporated until dry under high vacuum. The dried residue was completely dissolved in a mixture of  $\text{CDCl}_3$  and acetone- $d_6$  and 1,1,2,2-tetrachloroethane (106  $\mu\text{L}$ , 1 mmol) as a standard for calibration was added to the solution. The reaction conversions were determined from the ratio of proton signal of cyanohydrins at around 5.65 ppm and a signal from 1,1,2,2-tetrachloroethane at 5.95 ppm based on  $^1\text{H}$  NMR measurements.

### 2.5. Physical Measurements

NMR spectra were recorded on a Bruker Ascend 400 (400.13 MHz for  $^1\text{H}$ ) spectrometer.  $^1\text{H}$  chemical shifts were referenced to the proton resonance resulting from protic residue in deuterated solvent. The  $\text{N}_2$  and  $\text{CO}_2$  adsorption-desorption analyses were performed on a

Belsorp-miniII (BEL Japan) at 77 K and 196 K, respectively. The as-prepared MOF samples were dried at 150 °C or 180 °C for 2 h prior to measurement. Powder X-ray diffraction patterns were obtained using a Rigaku MiniFlex (30 kV, 15 mA, step size 0.02°). SEM images of gold-coated Cd-MOF were obtained on a Coxem CX-100S (accelerating voltage, 20 kV). Thermogravimetric analysis was carried out on a TGA Q5000 (TA Instruments) under a nitrogen atmosphere. FT-IR spectra in attenuated total reflection (ATR) mode were obtained on a Jasco FT/IR-4100 spectrometer. Elemental analysis was performed at the Organic Chemistry Research Center, Sogang University (Seoul, Korea) using EA1112 (CE Instruments, Italy).

### 2.6. X-ray Crystallography

The X-ray diffraction data for Co-MOF were collected on a Bruker D8 Venture diffractometer equipped with a Cu  $I\mu S^{\text{TM}}$  microfocus sealed-tube X-ray source ( $\lambda = 1.54178 \text{ \AA}$ ), and the diffraction data for Cd-MOF were collected on a Bruker APEX-II diffractometer. Each crystal was mounted on a glass fiber. The CCD data were integrated and scaled using the Bruker-S SAINT software package, and the structure was solved and refined using SHEXTL V6.12. All hydrogen atoms were placed in the calculated positions. The crystallographic data for the Co-MOF and Cd-MOF compounds are listed in Table 1. The selected bond distances are listed in Table 2. Structural information was deposited at the Cambridge Crystallographic Data Center (CCDC reference numbers are 961436 for Co-MOF and 961437 for Cd-MOF).

## 3. Results and Discussion

Co-MOF and Cd-MOF were prepared by thermal reactions of 1,4-H<sub>2</sub>NDC ligand with Co(NO<sub>3</sub>)<sub>2</sub>·6H<sub>2</sub>O and Cd(NO<sub>3</sub>)<sub>2</sub>·4H<sub>2</sub>O, respectively, in dimethylformamide (DMF). Solid-state structures of both MOFs are very similar to the general formula [M<sub>2</sub>(1,4-NDC)<sub>2</sub>(DMF)<sub>2</sub>] (M = Co<sup>II</sup> or Cd<sup>II</sup>) (Table 1 and 2). Both Co-MOF and Cd-MOF crystallized in the *P2<sub>1</sub>/c* space group, and the asymmetric unit consists of two metal ions, two 1,4-NDC, and two mutually *cis*-positioned DMF ligands. Both Co-MOF and Cd-MOF have similar cell dimensions, but the crystal quality of Cd-MOF gave us low quality data. The optical microscopic image of Cd-MOF is given in Fig. 1a. The morphology of the Cd-MOF crystals

is that of thin tapered needles which are grown from the same single root crystal. Also, the surfaces were not smooth. The surface structure of the crystals of Cd-MOF further investigated by scanning electron microscopy (SEM) indicated that many small particles covered the surfaces of rod shaped crystals (Fig. 1b and 1c). Thus, although we tried the preparation of Cd-MOF many times to obtain good single crystals with smooth surfaces, when preparing Cd-MOF, the same type of crystals were always obtained. Unexpectedly, however these crystals gave us diffraction data and we successfully solved the structure. Therefore, the crystals are thought to be a rare example of hierarchically ordered MOF. Otherwise, we could not have obtained a valid crystal structure. Because smaller crystals uniformly surround the rod shaped crystals as shown in Fig. 1c, the smaller crystals presumably epitaxially overgrew on the surfaces of the larger crystals [20].

1,4-NDC ligands bridge metal ions in chelating/bridging and simple bridging modes to form 1D chains, and these 1D chains are interconnected by 1,4-NDC ligands to form 3D frameworks (Fig. 2). There are two asymmetric metal ions with different coordination geometries: a metal ion adopted octahedral geometry, bound by four carboxylate oxygen atoms and two DMF oxygen atoms, and that of the other metal ion adopted pseudo-tetrahedral geometry, bound by two chelating carboxylates and two carboxylate oxygen atoms (Fig. 3). Two DMF ligands coordinate to only one of the two available metal ions in a mutually *cis*-positioned manner.

The purity of the bulk samples was checked by powder X-ray diffraction (PXRD) analysis. The PXRD patterns of the bulk as-prepared MOFs were compared with the simulated patterns based on the data obtained from X-ray crystallography as given in Fig. 4. The diffraction patterns of the as-prepared MOFs were in good agreement with those shown in the simulated data. Thus, the as-prepared MOFs are pure phases.

Thermogravimetric analysis (TGA) clearly suggested that the two DMF ligands in both as-prepared MOFs could be completely removed when suitably evacuated as shown in Fig. 5. As-prepared Co-MOF completely lost DMF ligands at 291 °C as shown in Fig. 5a. The corresponding first derivative curve indicates that a series of heat absorption occurred at 247, 278, and 463 °C. The first two heat absorption can be attributed to the removal of DMF ligands while the last heat absorption can be attributable to the decomposition of 1,4-NDC ligand. The as-prepared Cd-MOF exhibited heat absorption at 286, 379, and 432 °C as

depicted in Fig. 5b. The first heat absorption can be considered as complete removal of DMF ligands. Thus, the thermal stabilities of the two MOFs are slightly different.

Although PLATON analysis shows that the as-prepared MOFs are nonporous [21], the removal of the two DMF ligands would provide not only open metal sites but also void spaces. As depicted in Fig. 2, 1,4-NDC ligands are located alternately to leave no solvent accessible voids. This type of packing of 1,4-NDC ligands differs from the known grid-type of MOF having a mononuclear metal center and 1,4-BDC or N-donor based ditopic co-ligand. On the other hand, the porosity of the evacuated MOFs was estimated to be 29.6% for Co-MOF and 32.6% for Cd-MOF due to the removal of the two DMF ligands. The drying of the as-prepared Co-MOF at 180 °C under vacuum for 2 h afforded a DMF-free sample as evidenced by Fourier-transform infrared (FT-IR) absorption spectroscopy. The absorption band at 1653  $\text{cm}^{-1}$  for as-prepared Co-MOF can be attributed to the characteristic C=O stretching mode of the coordinated DMF ligands. The value is shifted into a lower wavenumber region upon coordination to  $\text{Co}^{\text{II}}$  metal ion compared with that of free DMF molecule, 1667  $\text{cm}^{-1}$ . The C=O stretching band of DMF ligands almost disappeared in the dried Co-MOF as depicted in Fig. 6. Despite this spectral change, the values of 1599 and 1407  $\text{cm}^{-1}$  for  $\nu(\text{COO}_{\text{asym}})$  and  $\nu(\text{COO}_{\text{sym}})$  of 1,4-NDC linkers in as-prepared Co-MOF remained without significant changes after drying. Furthermore, the FT-IR bands corresponding to the naphthyl ring were also observed for dried Co-MOF at 1534, 1461, 1360, 1262, 1212 and 775  $\text{cm}^{-1}$ . These results clearly suggest that the Co-1,4-NDC connectivity remained intact after the uncoordination of labile DMF ligands.

The gas sorption measurements were taken to investigate the permanent porosity of both MOFs. The  $\text{N}_2$  adsorption-desorption analyses of the evacuated MOFs at 180 °C or 230 °C did not show any meaningful sorption data at 77 K. Nevertheless, we also checked the  $\text{CO}_2$  sorption of the evacuated samples to test the  $\text{CO}_2$  sorption abilities of both MOFs at 196 K. Several flexible  $\text{CO}_2$ -selective MOFs exhibited  $\text{CO}_2$  sorption abilities despite their low sorption of  $\text{N}_2$  gases [22-25]. In both cases, however no meaningful sorption of  $\text{CO}_2$  was observed. The reason for this nonporosity may be attributed to either the collapse of frameworks or structural change into nonporous frameworks after the removal of the two labile DMF ligands which coordinate to the single metal ion. As the DMF ligands were eliminated, the coordination number of  $\text{M}(2)$  ion shown in Fig. 3a changed from six to four

and the stability of this metal center may not be high. Thus, we measured the PXRD patterns of the evacuated Co-MOF and Cd-MOF as shown in Fig. 4, and found that the evacuated MOFs almost lost their original crystallinity. Very weak diffraction planes of (020) and (040) were observed for both MOFs. Thus, neither of the MOFs showed permanent porosity upon evacuation due to the framework collapse.

Although neither of the MOFs exhibited meaningful sorption of N<sub>2</sub> and CO<sub>2</sub> due to their low porosities, the as-prepared Cd-MOF could be catalytically active for aldol-type reactions because it contains acidic Cd(II) ions with labile DMF ligands [26, 27]. Thus, we checked the catalytic activity of Cd-MOF for the cyanosilylation reaction of aromatic aldehydes with trimethylsilyl cyanide (TMSCN) in the presence of a catalytic amount of the as-prepared Cd-MOF (Fig. 7). The resulting cyanohydrins are very useful organic intermediate compounds for pharmaceuticals [18]. Three different aromatic aldehyde substrates were chosen for the comparison of reactivities: 4-nitrobenzaldehyde (4-NBA), 3-nitrobenzaldehyde (3-NBA), and 2-nitrobenzaldehyde (2-NBA). The corresponding reaction conversions are summarized in Fig. 7. We also examined the catalytic activities of as-prepared Co-MOF under the same reaction conditions. Unlike the Cd-MOF, however Co-MOF did not show significant activities for all three substrates.

Duan and co-workers recently reported a catalytically active porous lanthanide MOF, Tb-TCA, where H<sub>3</sub>TCA is tricarboxytriphenylamine, in which Lewis acidic openly accessible metal centers were available [28]. They investigated the catalytic activities of Tb-TCA for cyanosilylation reaction of 4-NBA, 3-NBA, and 2-NBA under the same experimental conditions. Interestingly, the conversions were increased in the order of 2-NBA (78%) > 3-NBA (59%) > 4-NBA (47%). They attributed the highest conversion of 2-NBA to the potential bidentate chelating ability of 2-NBA substrate to Tb ion compared with other NBA substrates. In general, 2-NBA and 4-NBA undergo faster reaction than 3-NBA in solution because of the favorable electronic effect of the 2- or 4-positioned electron-withdrawing nitro substituent. However, if the reaction mainly occurs inside the micropores, the reactivity trend could be altered due to the substrate shape and/or size-selection effect of the confined space [29-31]. For instance, Fujita and coworkers revealed that porous 2D Cd<sup>II</sup> network, [Cd(4,4'-bpy)<sub>2</sub>](NO<sub>3</sub>)<sub>2</sub> (4,4'-bpy = 4,4'-bipyridine), displayed substrate shape/size-dependent catalytic cyanosilylation [26]. The reaction conversion of 3-tolualdehyde (19%) was less than that of

2-tolualdehyde (40%). Furthermore, while 1-naphthaldehyde and 2-naphthaldehyde gave good conversions of 62% and 84%, respectively, the more sterically demanding substrate, 9-anthraldehyde, did not produce any product. Long and coworkers also demonstrated that microporous Mn<sup>II</sup>-containing MOF, Mn<sub>3</sub>[(Mn<sub>4</sub>Cl)<sub>3</sub>(BTT)<sub>8</sub>(CH<sub>3</sub>OH)<sub>10</sub>]<sub>2</sub> (H<sub>3</sub>BTT = 1,3,5-benzenetristetrazol-5-yl), displayed substrate-size dependent cyanosilylation reaction [32]. Both benzaldehyde (98%) and 1-naphthaldehyde (90%) gave higher conversions than 4-phenoxybenzaldehyde (19%) and 4-phenylbenzaldehyde (18%).

In our case, 4-NBA (49%) exhibited a higher conversion than 3-NBA and 2-NBA under the same reaction conditions. 2-NBA having an electronically favorable 2-positioned nitro group only exhibited negligible conversion (~ 1%), implying that the reaction mainly occurred inside the MOF pores. The reaction conversion of 2-NBA was even lower than 3-NBA. Each benzaldehyde contains nitro substituents at systematically varied positions as depicted in Fig. 8. The shape and dimensions are also indicated in Fig. 8. The molecular shapes of both 3-NBA and 2-NBA approximate a square geometry, while 4-NBA displays a rectangular geometry. The physical dimension of 2-NBA is slightly larger than that of 3-NBA. This difference may account for the higher reaction conversion of 3-NBA than 2-NBA. Therefore, the reaction conversions are strongly dependent on both the shape and dimension of the aldehyde substrates. In order to further confirm that the reaction actually occurs inside the Cd-MOF micropores, we analyzed the Connolly surface of DMF-free Cd-MOF as shown in Fig. 9. The shape of the accessible micropores is a flat rectangular geometry along the *b*-axis as depicted in Fig. 9b and 9c. Thus, 4-NBA is the most suited substrate for the catalytic reaction. The pores along the *c*-axis are not fully accessible as depicted in Fig. 9d and 9e. Although the framework of evacuated Cd-MOF collapsed, the as-prepared Cd-MOF in solution may provide catalytic Cd<sup>II</sup> active sites through partial dissociation of DMF ligands. This partial dissociation of DMF ligands near the surfaces of Cd-MOF particles may prevent the framework collapse. Therefore, the catalytic cyanosilylation reaction mainly occurs on the surfaces of Cd-MOF. It is interesting to note that such surface reaction is still sufficient to lead to substrate shape- and size-dependent catalysis.

#### 4. Conclusion

New 3D Co-MOF and Cd-MOF containing rigid 1,4-NDC bridging ligands were prepared and structurally characterized. Both 3D MOFs are isostructural and contain two asymmetric metal ions with different coordination geometries. One metal ion adopted octahedral bound by four carboxylate oxygen atoms and two DMF oxygen atoms, and the other adopted pseudo-tetrahedral bound by two chelating carboxylates and two carboxylate oxygen atoms. Two DMF ligands coordinate to only one of the two available metal ions in a mutually *cis*-positioned manner. These two DMF ligands could be thermally removed under vacuum to lead MOFs with openly accessible Lewis acidic metal sites. Single crystals of Cd-MOF exhibited rare hierarchical particle morphology. Small crystals epitaxially overgrew on a large crystal. The as-prepared Cd-MOF displayed catalytic activity in cyanosilylation of aromatic aldehydes due to the acidic metal centers once the labile DMF ligands dissociate from Cd<sup>II</sup> ions in solution. The heterogeneous cyanosilylation reaction mainly occurred inside the Cd-MOF micropores along the *b*-axis generated through the partial dissociation of DMF ligands near the surfaces of Cd-MOF. The reaction yields were strongly dependent on the shape and dimension of the aldehyde substrates.

### Acknowledgments

The Basic Science Research Program through the National Research Foundation of Korea (NRF), funded by the Ministry of Education, Science and Technology (NRF-20110008018, 2013R1A1A2006914, 2015R1D1A1A01058136), and the Gyeonggi Regional Research Center (GRRC) Program of Gyeonggi Province (GRRC-HUFS-2015-B04), and Financial support from Kwangwoon University in the year 2015 are gratefully acknowledged.

### Appendix A. Supplementary material

CCDC 961436 and 961437 contain the supplementary crystallographic data for this paper. These data can be obtained free of charge from The Cambridge Crystallographic Data Centre via [www.ccdc.cam.ac.uk/data\\_request/cif](http://www.ccdc.cam.ac.uk/data_request/cif).

**References**

- [1] H. Li, M. Eddaoudi, M. O'Keeffe, O. M. Yaghi, *Nature* 402 (1999) 276-279.
- [2] H. Furukawa, K. E. Cordova, M. O'Keeffe, O. M. Yaghi, *Science* 341 (2013) 1230444-1 - 1230444-12.
- [3] S. Huh, T.-H. Kwon, N. Park, S.-J. Kim, Y. Kim, *Chem. Commun.* (2009) 4953-4955.
- [4] N. L. Rosi, J. Eckert, M. Eddaoudi, D. T. Vodak, J. Kim, M. O'Keeffe, O. M. Yaghi, *Science* 300 (2003) 1127-1129.
- [5] A. Sonnauer, F. Hoffmann, M. Fröba, L. Kienle, V. Duppel, M. Thommes, C. Serre, G. Férey, N. Stock, *Angew. Chem. Int. Ed.* 48 (2009) 3791-3794.
- [6] X.-F. Wang, Y.-B. Zhang, W.-X. Zhang, W. Xue, H.-L. Zhou, X.-M. Chen, *CrystEngComm* 13 (2011) 4196-4201.
- [7] I. Senkowska, J. Fritsch, S. Kaskel, *Eur. J. Inorg. Chem.* (2007) 5475-5479.
- [8] S. S. Nagarkar, A. K. Chaudhari, S. K. Ghosh, *Inorg. Chem.* 51 (2012) 572-576.
- [9] T. Loiseau, C. Mellot-Draznieks, H. Muguerra, G. Férey, M. Haouas, F. Taulelle, C. R. Chimie. 8 (2005) 765-772.
- [10] Z. Wang, C.-M. Jin, T. Shao, Y.-Z. Li, K.-L. Zhang, H.-T. Zhang, X.-Z. You, *Inorg. Chem. Commun.* 5 (2002) 642-648.
- [11] D. T. Vodak, M. E. Braun, J. Kim, M. Eddaoudi, O. M. Yaghi, *Chem. Commun.* (2001) 2534-2535.
- [12] T. Loiseau, C. Serre, C. Huguenard, G. Fink, F. Taulelle, M. Henry, T. Bataille, G. Férey, *Chem. Eur. J.* 10 (2004) 1373-1382.
- [13] L. Wang, K. Zhang, T. Song, C. Li, J. Xu, L. Wang, *Micropor. Mesopor. Mater.* 155 (2012) 281-286.
- [14] J. L. Harding, M. M. Reynolds, *J. Am. Chem. Soc.* 134 (2012) 3330-3333.
- [15] A. Dhakshinamoorthy, M. Alvaro, H. Garcia, *Chem. Commun.* 48 (2012) 11275-11288.
- [16] M. Yoon, R. Srirambalaji, K. Kim, *Chem. Rev.* 112 (2012) 1196-1231.
- [17] A. H. Chughtai, N. Ahmad, H. A. Younus, A. Laypkovc, F. Verpoort, *Chem. Soc. Rev.* 44 (2015) 6804-6849.
- [18] M. North, D. L. Usanov, C. Young, *Chem. Rev.* 108 (2008) 5146-5226.
- [19] K. Mo, Y. Yang, Y. Cui, *J. Am. Chem. Soc.* 136 (2014) 1746-1749.
- [20] T.-J. M. Luo, J. C. MacDonald, G. T. R. Palmore, *Chem. Mater.* 16 (2004) 4916-4927.

- [21] A. L. Spek, PLATON – A Multipurpose Crystallographic Tool, Utrecht University, Utrecht, The Netherlands, 2004.
- [22] I. H. Hwang, J. M. Bae, Y.-K. Hwang, H.-Y. Kim, C. Kim, S. Huh, S.-J. Kim, Y. Kim, Dalton Trans. 42 (2013) 15645-15649.
- [23] I. H. Hwang, H.-Y. Kim, M. M. Lee, Y. J. Na, J. H. Kim, H.-C. Kim, C. Kim, S. Huh, Y. Kim, S.-J. Kim, Cryst. Growth Des. 13 (2013) 4815-4823.
- [24] J. Zhang, H. Wu, T. J. Emge, J. Li, Chem. Commun. 46 (2010) 9152-9154.
- [25] S. Henke, R. Schmid, J.-D. Grunwaldt, R. A. Fischer, Chem. Eur. J. 16 (2010) 14296-14306.
- [26] M. Fujita, Y. J. Kwon, S. Washizu, K. Ogura, J. Am. Chem. Soc. 116 (1994) 1151-1152.
- [27] D. Dang, P. Wu, C. He, Z. Xie, C. Duan, J. Am. Chem. Soc. 132 (2010) 14321-14323.
- [28] P. Wu, J. Wang, Y. Li, C. He, Z. Xie, C. Duan. Adv. Funct. Mater. 21 (2011) 2788-2794.
- [29] J.-M. Gu, W.-S. Kim, S. Huh, Dalton Trans. 40 (2011) 10826-10829.
- [30] Y. Zhao, K. Chen, J. Fan, T.-a. Okamura, Y. Lu, L. Luoa, W.-Y. Sun, Dalton Trans. 43 (2014) 2252-2258.
- [31] M. Yoshizawa, M. Tamura, M. Fujita, Science 312 (2006) 251-254.
- [32] S. Horike, M. Dincá, K. Tamaki, J.R. Long, J. Am. Chem. Soc. 130 (2008) 5854-5855.

Table 1. Crystallographic Data for Co-MOF and Cd-MOF.

	Co-MOF	Cd-MOF
Empirical formula	$C_{30}H_{26}Co_2N_2O_{10}$	$C_{30}H_{26}Cd_2N_2O_{10}$
Formula weight	692.39	799.33
Temperature (K)	100(2)	170(2)
Wavelength (Å)	1.54178	0.71073
Space group	$P2_1/c$	$P2_1/c$
a (Å)	7.0771(2)	7.2030(14)
b (Å)	19.3930(7)	19.888(4)
c (Å)	19.6397(6)	19.968(4)
$\alpha$ (°)	90.00	90.00
$\beta$ (°)	97.168(2)	94.94(3)
$\gamma$ (°)	90.00	90.00
Volume(Å <sup>3</sup> )	2674.41(15)	2849.9(10)
Z	4	4
Density (calc.) (Mg/m <sup>3</sup> )	1.720	1.863
Absorption coeff. (mm <sup>-1</sup> )	10.305	1.556
Crystal size (mm <sup>3</sup> )	0.10 × 0.03 × 0.02	0.15 × 0.08 × 0.02
Reflections collected	16209	16490
Independent reflections	2062 [R(int) = 0.0745]	6272 [R(int) = 0.1488]
Data/restraints/parameters	2062 / 7 / 401	1272 / 15 / 363
Goodness-of-fit on F <sup>2</sup>	1.043	0.996
Final R indices [I>2σ(I)]	R <sub>1</sub> = 0.0401, wR <sub>2</sub> = 0.0935	R <sub>1</sub> = 0.1307, wR <sub>2</sub> = 0.3200
R indices (all data)	R <sub>1</sub> = 0.0508, wR <sub>2</sub> = 0.0994	R <sub>1</sub> = 0.2101, wR <sub>2</sub> = 0.3519
Largest diff. peak and hole (e.Å <sup>-3</sup> )	0.796 and -0.536	3.944 and -1.869

Table 2. Selected Bond Distances for Co-MOF and Cd-MOF.

	Co-MOF	Cd-MOF
M-O <sub>carboxylate</sub>	2.008(4)-2.279(4)	2.232(14)-2.379(10)
M-O <sub>DMF</sub>	2.105(5), 2.2112(7)	2.248(13), 2.262(17)
M···M	3.845, 3.876	3.925, 4.024

ACCEPTED MANUSCRIPT

## Figure Captions

**Fig. 1.** Optical microscopy image of Cd-MOF (a). SEM images of hierarchical Cd-MOF crystals at different magnifications. Image (c) is the enlarged view of the square outlined area of (b).

**Fig. 2.** Framework structure of Co-MOF and Cd-MOF containing 1,4-NDC shown along the *a*-axis. Hydrogen atoms are omitted for clarity.

**Fig. 3.** Asymmetric unit of Co-MOF and Cd-MOF (a). Crystal structure of the asymmetric unit of Co-MOF with atomic labelling scheme (b). Displacement ellipsoids are shown at the 50% probability level. All hydrogen atoms were omitted for clarity. Symmetry operations: (i)  $-x, 0.5+y, 0.5-z$ , (ii)  $-x, -0.5+y, 0.5-z$ , (iii)  $-1+x, y, z$ , (iv)  $1+x, y, z$ , (v)  $1+x, 1.5-y, 0.5+z$ , and (vi)  $-1+x, 1.5-y, -0.5+z$ .

**Fig. 4.** Comparison of the PXRD patterns of the as-prepared MOFs, simulated data, and dried MOFs. Co-MOF (a) and Cd-MOF (b).

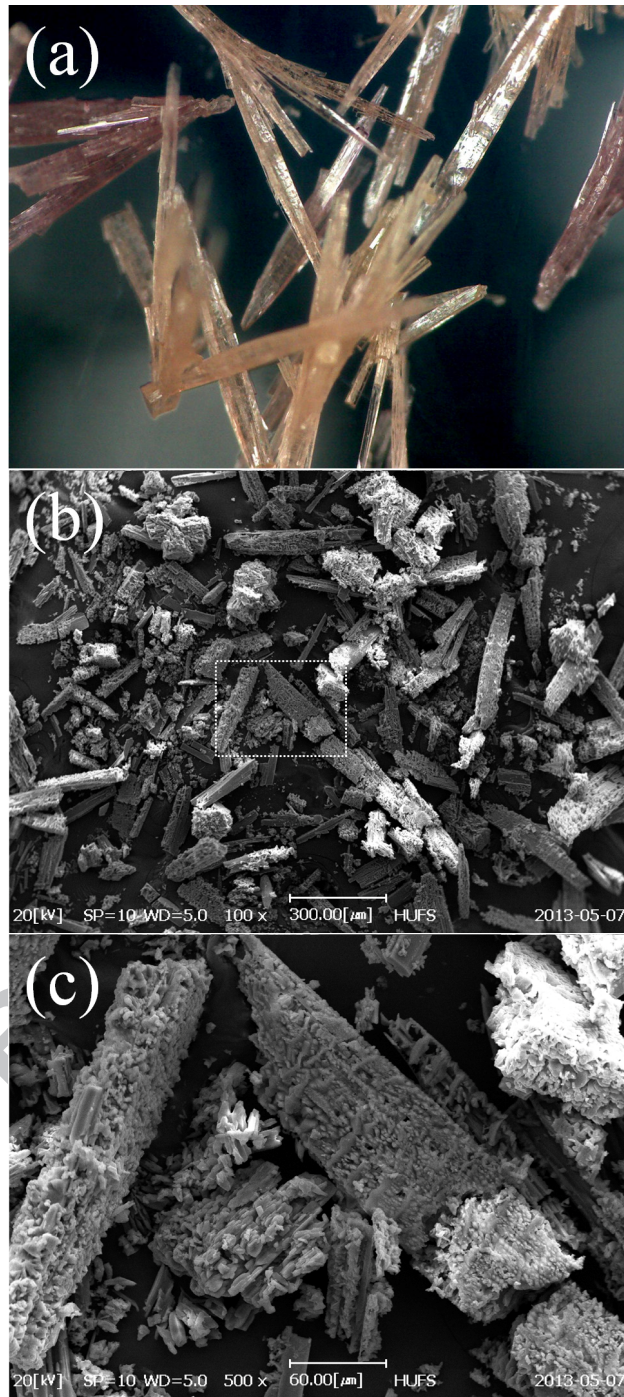
**Fig. 5.** TG curves and their first derivatives for the as-prepared Co-MOF (a) and Cd-MOF (b).

**Fig. 6.** FT-IR spectra of the as-prepared Co-MOF (solid line in blue) and evacuated Co-MOF (dotted line in red).

**Fig. 7.** Substrate-dependent reaction conversions in the cyanosilylation reaction of aromatic aldehydes catalyzed by the as-prepared Cd-MOF. Reaction conditions: as-prepared Cd-MOF, 20 mg; substrate, 1.0 mmol; TMSCN, 1.0 mmol; 50°C (3 d).

**Fig. 8.** Comparison of the molecular dimensions of aldehyde substrates. In order to estimate the physical dimensions of these molecules, we chose two suitable atoms and calculated their center-to-center distance using Chem3D then added their van der Waals radii.

**Fig. 9.** Connolly surface of DMF-free Cd-MOF probed with a probe radius of 1.0 Å along the *a*-axis (a), the same Connolly surface viewed down the *b*-axis (b), and *c*-axis (d). The corresponding ball-and-stick framework structures (c, e). Grey and green colors in (a), (b), and (d) indicate the exterior and interior of the surface, respectively.

**Fig. 1**

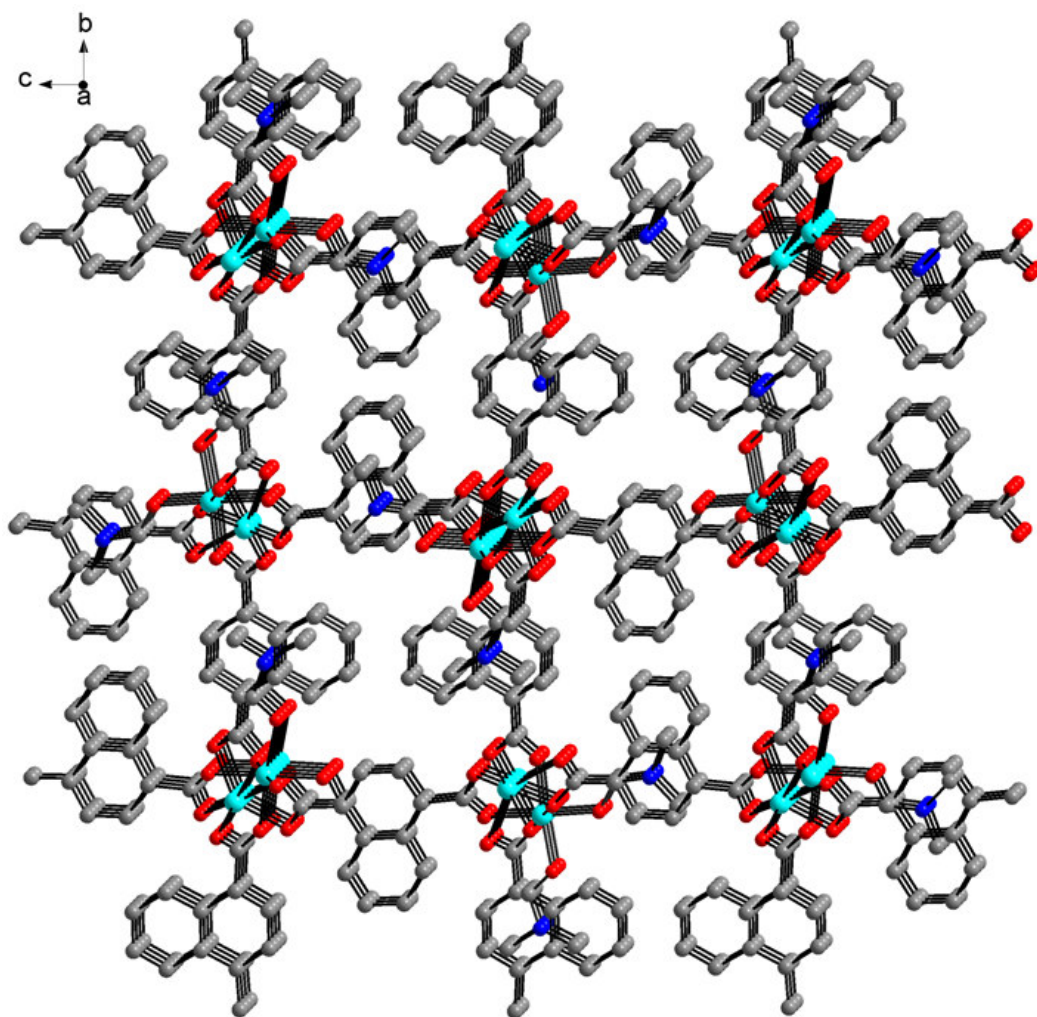
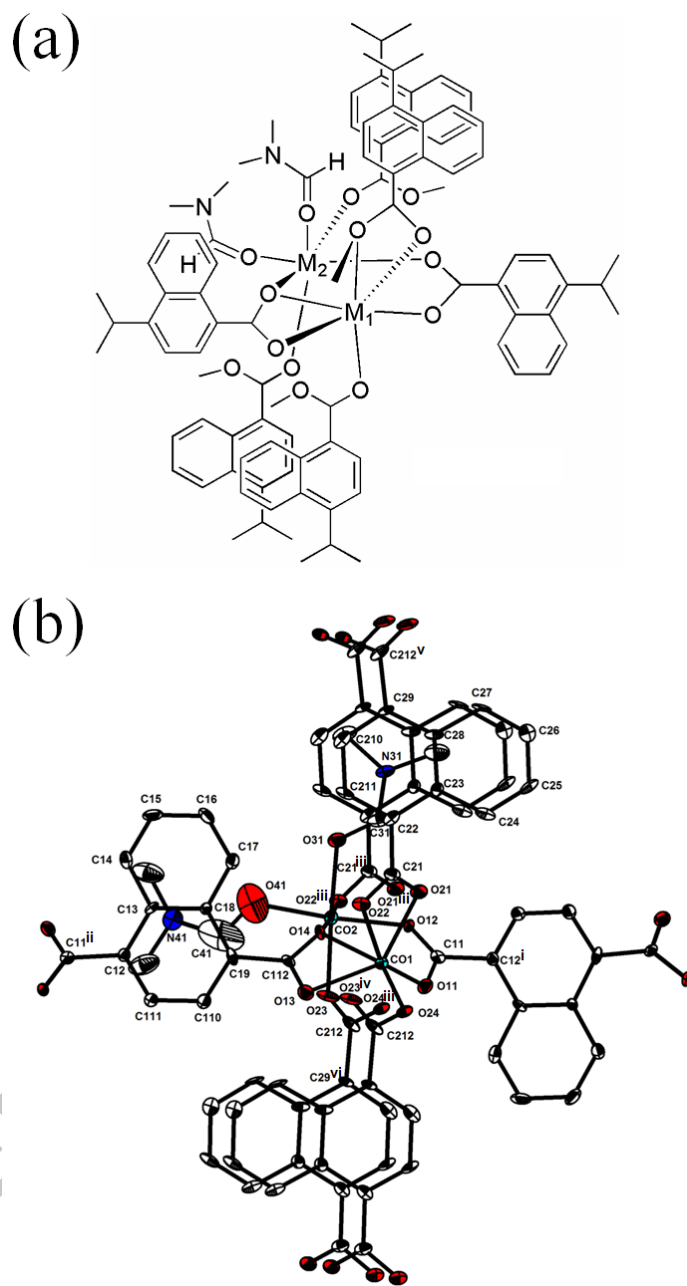


Fig. 2



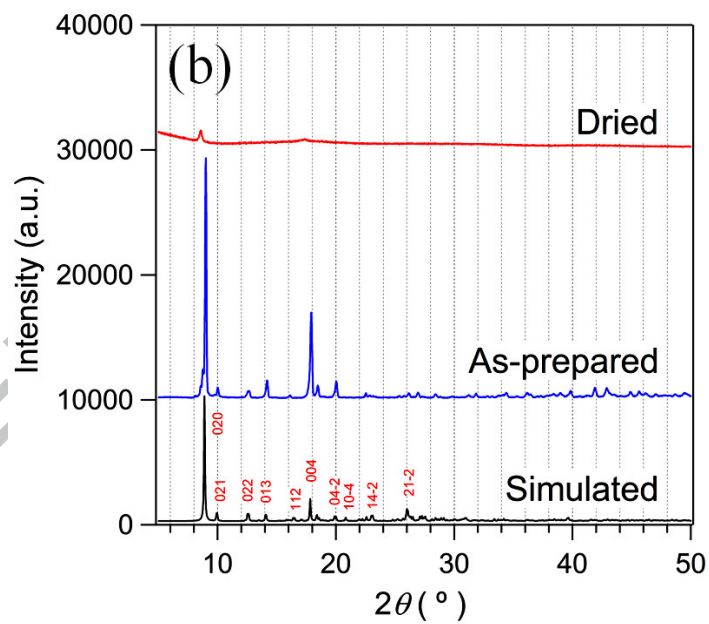
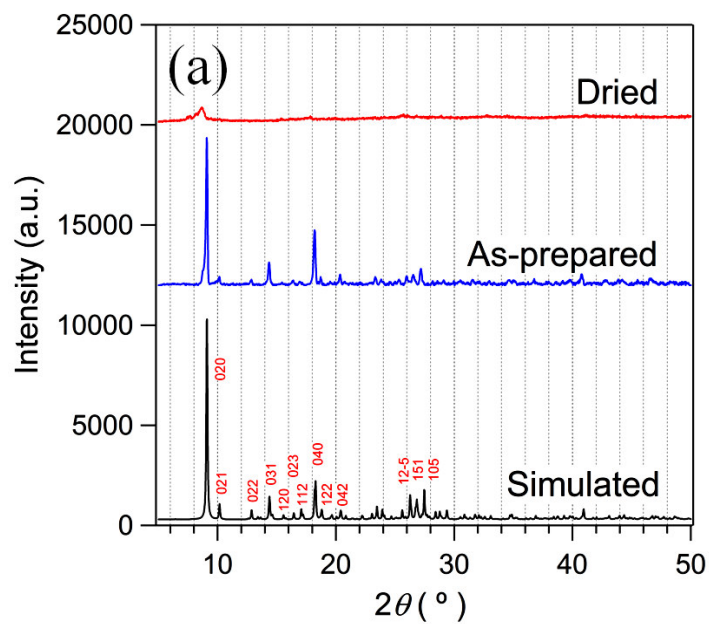


Fig. 4

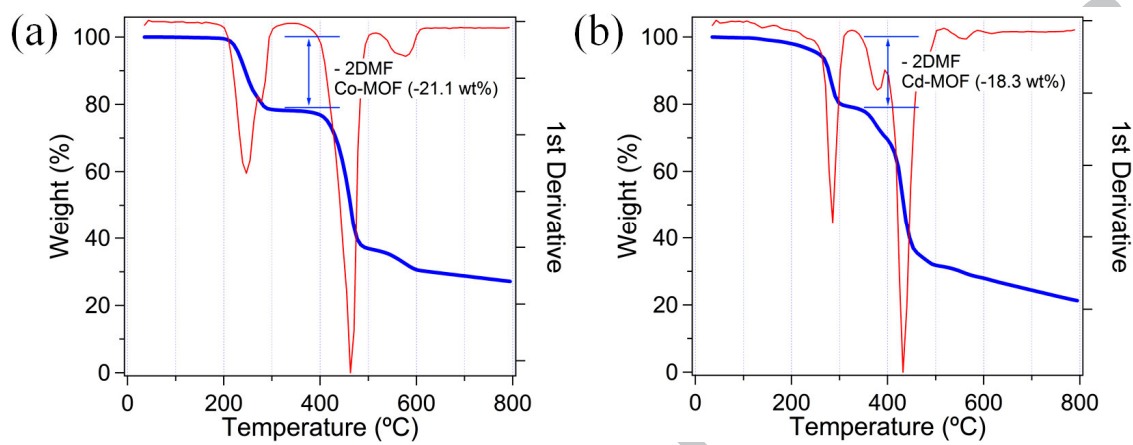


Fig. 5

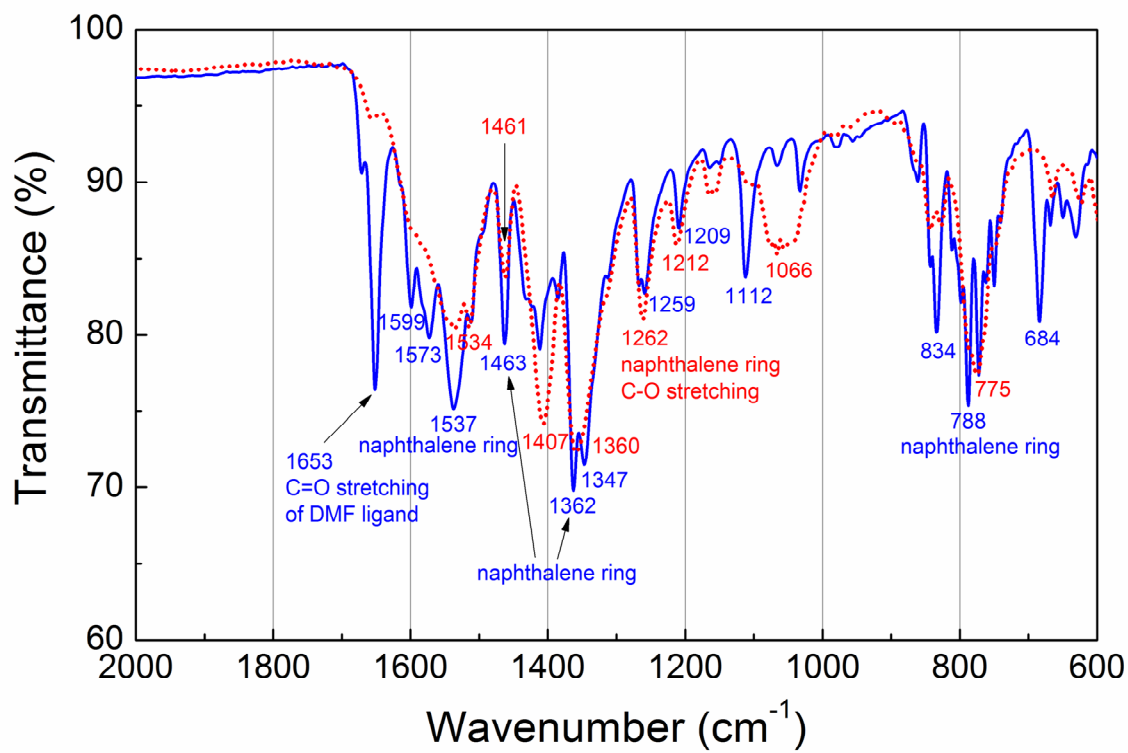


Fig. 6

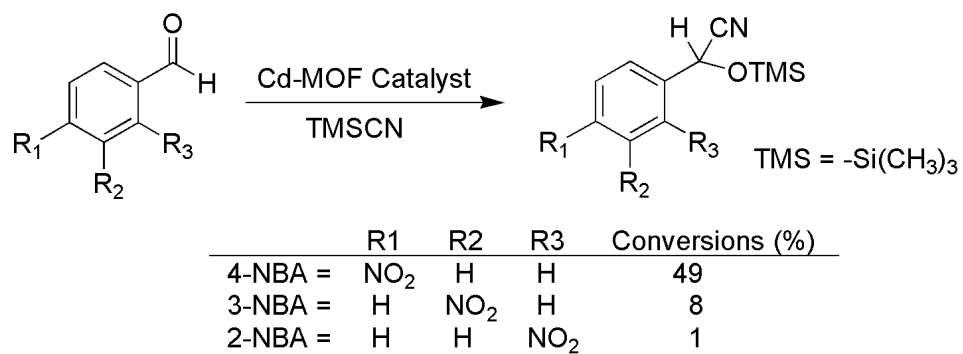


Fig. 7

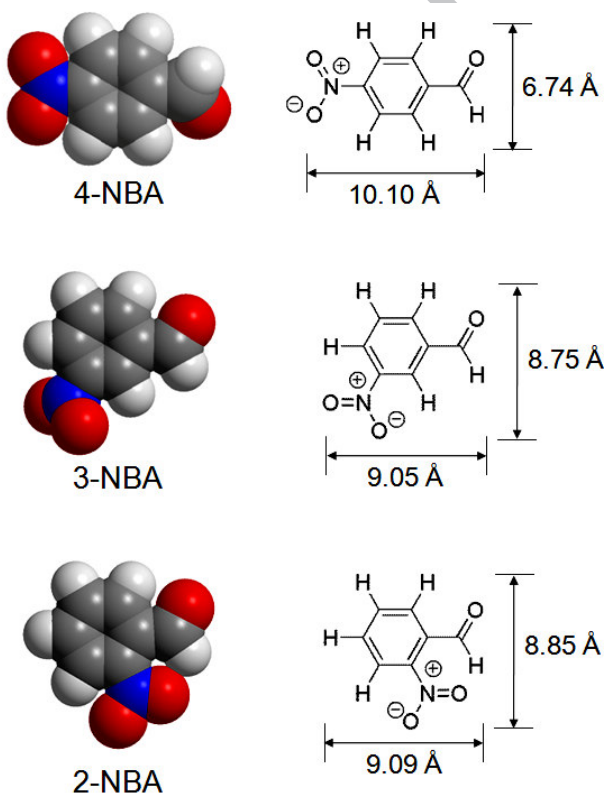


Fig. 8

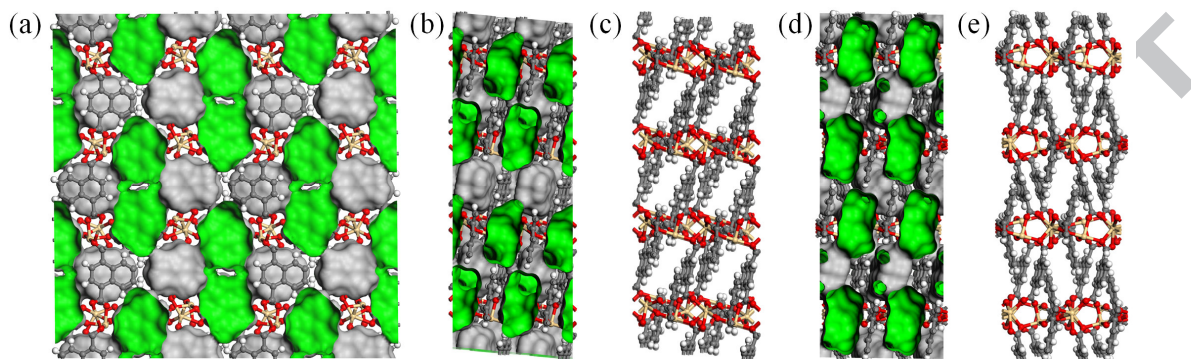


Fig. 9

*Graphical Abstract***Three-Dimensional Cobalt(II) and Cadmium(II) MOFs Containing 1,4-Naphthalenedicarboxylate: Catalytic Activity of Cd-MOF**

In-Hwan Choi, Youngmee Kim, Do Nam Lee\*, and Seong Huh\*

3D metal-organic frameworks with the formula of  $[M_2(1,4\text{-NDC})_2(\text{DMF})_2]$  ( $M = \text{Co}^{\text{II}}$  or  $\text{Cd}^{\text{II}}$ ) were formed, and the as-prepared Cd-MOF was found to be catalytically active for the cyanosilylation reaction of aromatic aldehydes with nitro substituent in varying positions in the presence of trimethylsilyl cyanide to afford cyanohydrin trimethylsilyl ethers in a shape and size selective manner.

